

# RECENT DEVELOPMENTS IN 2D NANOMATERIALS FOR SUPERCAPACITOR APPLICATIONS

## Abstract

Recently discovered two-dimensional (2D) nanomaterials ensure exceptional chemical and physical capabilities, particularly electrochemical properties, due to their superior inherent and exterior forms. As a result, they are emerging as very desired candidates for energy conservation devices such as supercapacitors. The most recent advancements in 2D nanomaterials for conductive energy reserve are summarised in this study. Production techniques for 2D nanomaterials such as graphene, transition metal oxides, dichalcogenides, and carbides, in addition to their electrochemical characteristics, are reviewed. The approaches used to construct 2D graphene, among other materials, increase the performance of electrodes, and hence the overall charge discharge. It is specifically discussed how to design 2D and 3D architectures that are blended and multilayered utilising 2D nanomaterials. The positive aspects along with drawbacks of employing supercapacitors which use 2D nanomaterials are examined. We discuss recent progress in converting several 2D nanomaterials, particularly graphene, into 3D materials for usage in supercapacitors. The investigation of Energy-storage materials based on graphene begins with an examination of the electric double-layer charging and discharging mechanism, which is prevalent in these materials. However, when doped or chemically functionalized graphene is utilised, the pseudocapacitive process is also covered. Following that, non-carbon 2D nanomaterials are examined, includes pseudocapacitive processes for ion intercalation and redox mechanisms taking precedence. Transition metal carbides, transition metal dichalcogenides, and metal oxides are examples of these. The approaches for combining 3D enormous materials from two-dimensional nanomaterials, which are critical for creating various devices, are then discussed.

**Keywords:** 2D –Transition metal dichalcogenides, 3D Graphene, Functionalization, Energy Storage, Supercapacitors

## Authors

### **Thushara. K. M**

Department of Applied  
Science & Humanities  
Nehru College of Engineering  
& Research Centre  
Thrissur, Kerala, India.

### **R. Lakshmi**

Assistant Professor  
Department of Chemistry  
T. John Institute of Technology  
Bangalore, Karnataka, India.

### **Dr. K. Rajalakshmi**

Assistant Professor  
Department of Chemistry  
Shrimati Indira Gandhi College  
Affiliated to Bharathidasan  
University  
Tiruchirapalli, Tamil Nadu, India.

### **Dr. B. Varalakshmi**

Assistant professor  
Department of Biochemistry  
Shrimati Indira Gandhi college  
Affiliated to Bharathidasan  
University  
Tiruchirapalli, Tamil Nadu, India.

## I. INTRODUCTION

Due to the growing demand across many industries over the last few decades, energy storage research has become very popular. The reasons for the intense attention being paid to energy storage, namely the use of nanomaterials in super capacitors, are based on the properties of materials with improved ionic diffusion. Interest in graphene and its derivatives has increased in this field owing to its specifications such as Tunable surface area, weightless, exceptional chemical stability and electrical conductivity environment friendly and easily accessible. Starting with a description of the process for charging and discharging electronic devices in two layers which is prevalent in these materials, the research of energy-storage materials built on graphene and its variants are introduced. Nonetheless, the usage of doped or chemically functionalized graphene also covers the pseudocapacitive mechanism. In the discussion of non-carbon 2D nanomaterials that follows, pseudo capacitive mechanisms based on redox and ion intercalation predominate. They consist of transition metal dichalcogenides, transition metal carbides, and metal oxides. The methods for combining 3D macro materials utilizing 2D nanomaterials—which are essential for developing various devices—are next covered.

- 1. Graphene:** An infinite 2D crystal made of sp<sup>2</sup>-hybridized carbon atoms with an atomic thickness is referred to as graphene. Graphene has a potential aggregate surface area of 2630 m<sup>2</sup>g<sup>-1</sup>. It is promising for storage of electricity requirements considering its exceptional electronic characteristics [1-5]. Graphene layers' chemical characteristics, texture, structural flaws, pore size, shape, and orientation have all been investigated thus far. Relevant properties and the processes used to create them are tightly related. Chemical vapour deposition (CVD), physical or chemical exfoliation [Fig.1.1] and decrease in graphite oxide concentration are techniques that can be used to make graphene. Raman spectroscopy shows that low lattice defect levels are present in CVD (ID/IG = 0.67, peak D to peak G intensity ratio), which conserves strong conductivity of electricity [6-9]. In a KOH/water electrolyte at a frequency of 120 Hz, a symmetric device with a 4cm<sup>2</sup> geographic region displayed areal capacitance is minimal of 97.5 Fcm<sup>-2</sup> but a quick capacitor sensitivity to 8.3ms, which corresponded to -83 degree impedance phase angle. The solvent serves as a source of the sufficient superficial drive required to avoid post exfoliation agglomeration when exfoliating graphite in liquid phase exfoliation, which uses using the force of ultrasonic vibrations to cut through graphite layers that are submerged in a solution [10,11]. Pseudo capacitance and double-layer capacitance were displayed by the graphene electrodes.

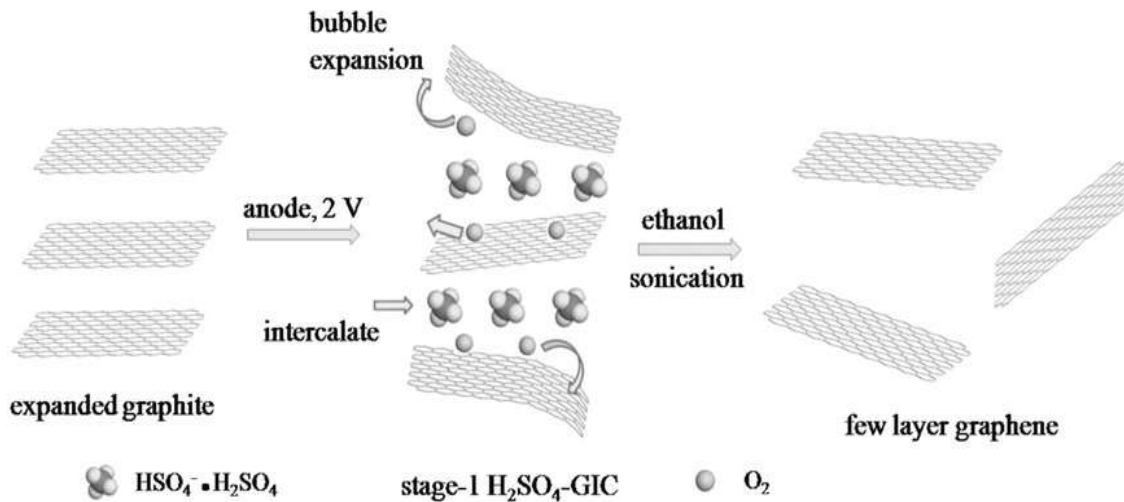


**Figure 1.1:** A significant phase in the production of few layer grapheme

Hummer techniques are commonly used to create chemically reduced graphene oxide (CRGO). It is then decreased by means of a synthetical agent after being exfoliated in water [12,13]. On its basal planes and edges, graphene oxide (GO) often has a variety of chemical features, including groups such as carbonyl, carboxyl, epoxide, and hydroxyl [14]. The reduction step eliminates the majority of chemical properties and replenishes the graphene lattice, but typically leaves behind some chemical functionalities and structural flaws. In a tetraethyl ammonium tetrafluoroborate acetonitrile electrolyte, CRGO composed of 15 to 20 nm nanoparticles produced electrical conductivities of 200 S/m and capacitances of 100 F/g [12].

- Two-Dimensional Transition Metal Dichalcogenide:** A wide class of 2D nanomaterials called transition metal dichalcogenides includes both metallic and semiconducting nanomaterials. The most utilised transition metal dichalcogenide among them is MoS<sub>2</sub>, which exhibits polytypes of 2H (semiconducting), 1T (metal) and 3R (stable within typical circumstances) [15]. By intercalating Lithium-ions within the majority of MoS<sub>2</sub>, trailed by exfoliation in water [16,17], 2D MoS<sub>2</sub> can be created chemically or electrochemically [18-20]. Chhowalla et al. demonstrated that chemical exfoliation produced 100% monolayer MoS<sub>2</sub>, and that after Li-ion intercalation, around 70% of the material changed from the 2H to the 1T phase.
- Three-Dimensional Graphene:** Integrated structures can be created by combining 2D graphene with electrochemically active materials after being constructed into a 3D macroscopic structure. New 2D Nanomaterials for Applications in Supercapacitors For supercapacitors, see Chapter J. 5 157. Fast ion and electron transfer encouraged by the 3D linked network. Additional benefits of graphene-based 3D designs include their flexibility and light weight. Because of their light weight, graphene and its derivatives can efficiently lower the substrate's mass ratio and increase the electrode's overall power/energy density. Additionally, the very porous structure of 3D graphene networks can speed up reaction kinetics, resulting in higher energy/power densities. Due to these outstanding qualities, research on high-performance supercapacitors is now paying more attention to 3D graphene-based integrated electrodes. The following techniques can be used to create 3D graphene designs. As illustrated in Fig. 1.2, 3D

graphene structures were created by Dai et al. using a 3D copper mesh. Frameworks of 3D graphene synthesised through CVD is made by the catalytic degradation of miniature organic molecules, or hydrocarbons the use of catalytic transition metals, such as Ni [21,22]. Due to its excellent quality and low defect count, CVD is now the most widely used approach for the creation of self-supporting 3D graphene structures, particularly for self supported graphene foam (GF) [23-26]. As of its adjustable pore size and 3D periodic morphologies, colloidal lithography can furthermore be utilised to build 3D graphene architectures, as shown in Fig. 1.3.

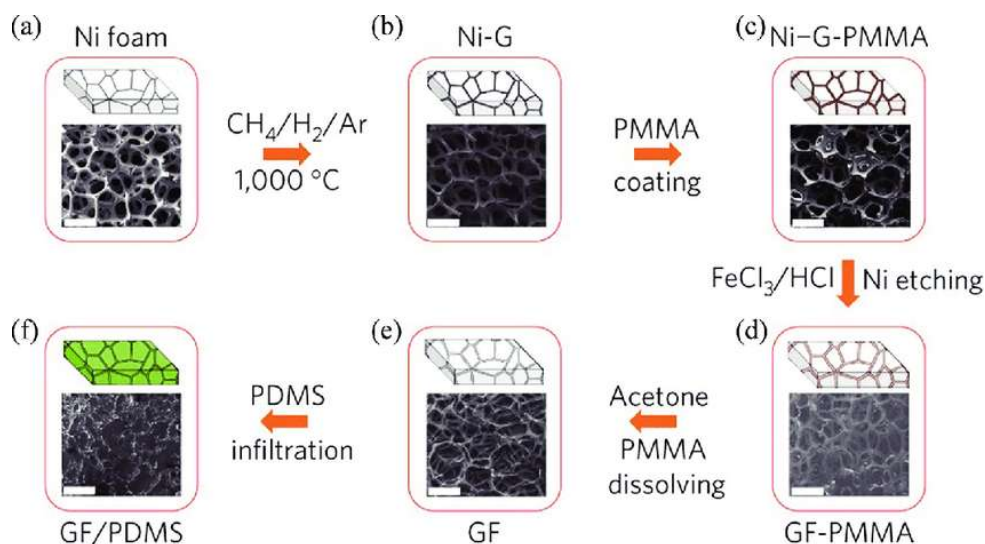


**Figure 1.2:** Graphene foam (GF) fabrication and incorporation with polydimethylsiloxane (PDMS).

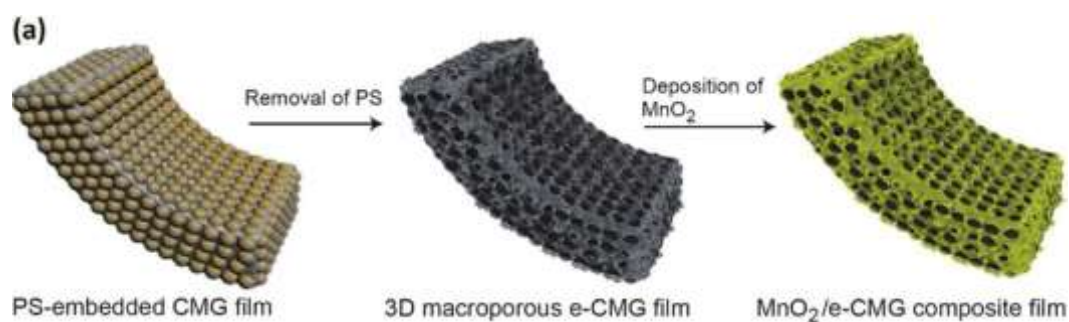


**Figure 1.3:** Graphene foam production utilising a polystyrene spherical (PS) template, shown schematically in (a)

## II. METHODS OF SYNTHESIS

By electrochemically intercalating and exfoliating extended graphite (EG) in  $\text{H}_2\text{SO}_4$  electrolyte, few-layer graphene (FLG) was created [27]. Electrochemical electrode constructed from EG was pressed into a plate. EIE was performed using In a 10 M  $\text{H}_2\text{SO}_4$  electrolyte, pt foil serves as the counter-electrode. Low voltage of 1 V was applied to the EG electrode for 10 minutes while using stage 1  $\text{H}_2\text{SO}_4$ -graphite intercalation compound

(intermediate A). After that, the preference was ramped up to 2 V for 20 minutes. Milli-Q water was used to completely wash the resultant sample. The water-washed sample was then subjected to a 10-minute ultrasonic treatment in ethanol to create graphenenanosheets. More than 90% of the starting ingredients were used to produce the exfoliated FLG flakes.

GO dispersion underwent hydrothermal treatment to produce GF. A simple roll-forming approach was used to combine nickel foam (NF) with hybrid graphene/Ni foam (HGNF). By applying cyclic voltammetry (CV) techniques, Manganese dioxide and polyaniline remained electrooxidatively and electropolymerizably dropped onto Hybrid Graphene Nickel Foam, respectively. MnO<sub>2</sub>/HGNF and PANI/HGNF were used as the positive and negative electrodes, correspondingly, in the construction of a flexible asymmetric supercapacitor (ASC) [28]. A previously described procedure [55] was followed in the preparation of the Cu<sub>2</sub>O cubes. The resulting CuO samples were first liquefied in 10 mL of purified water and then ultrasonically agitated for around 30 minutes. The resultant liquid was then added to a 40 mL solution of 0.125 M Na<sub>2</sub>C<sub>2</sub>O<sub>4</sub>. The combined solution was then centrifuged after being vigorously agitated at ambient temperature for five hours. The Na<sub>2</sub>C<sub>2</sub>O<sub>4</sub>-treated CuO cubes were sonicated for at a constant temperature for 30 minutes to disseminate them in deionized water. The required quantity of dopamine (DA) was then incrementally supplementary to the floating system, agitated for 24 hours, and then centrifuged. The dried material was mixed vigorously with a 10 M Tris hydrochloride solution twelve hours of time at room temperature. The polydopamine (PDA)-modified CuO nanocrystals, abbreviated as PDA/CuO, were produced employing agitation repeatedly washed with deionized water. The PDA/CuO sample was then vacuum-sealed to dry for 24 hours at 70 degree celcius

### III. RESULTS AND DISCUSSION

**1. Two-dimensional Graphene and Graphene paper are Synthesis using an Electrochemical Method:** Pictures of the a few-layered 2D sheets of graphene were formed in the form of powders are shown in Fig. 1.4(a). Graphene emulsion at a concentration of 0.5 mg mL<sup>-1</sup> in N-methyl-2-pyrrolidone can remain stable for two months, as illustrated in Fig. 1.4(a). The resulting graphenenanosheets are depicted in typical scanning electron microscopy (SEM) pictures in Fig. 1.4B and C. We can see morphologies like rumpling and scrolling that are typical of extremely thinnanosheets of graphene. HRTEM pictures of Fig. 1.4B demonstrate that the margins of the graphenenanosheets are composed of trilayers, bilayers, or both. According to statistics, The majority of graphenenanosheets (83%) are ultrathin nanosheets since their thickness is fewer than seven layers. By placing a silicon substrate in contact with a dispersion solution, exfoliated graphenenanosheets may be seen in Fig. 1.6A as representative atomic force microscopy (AFM) photographs. Less than 3 nm is the reported thickness of 78 of the 92 pieces of graphenenanosheets based on the AFM height profiles. Accordingly, 85% of graphenenanosheets have seven or fewer layers, which is consistent with the conclusions of transmission electron microscopy (TEM).

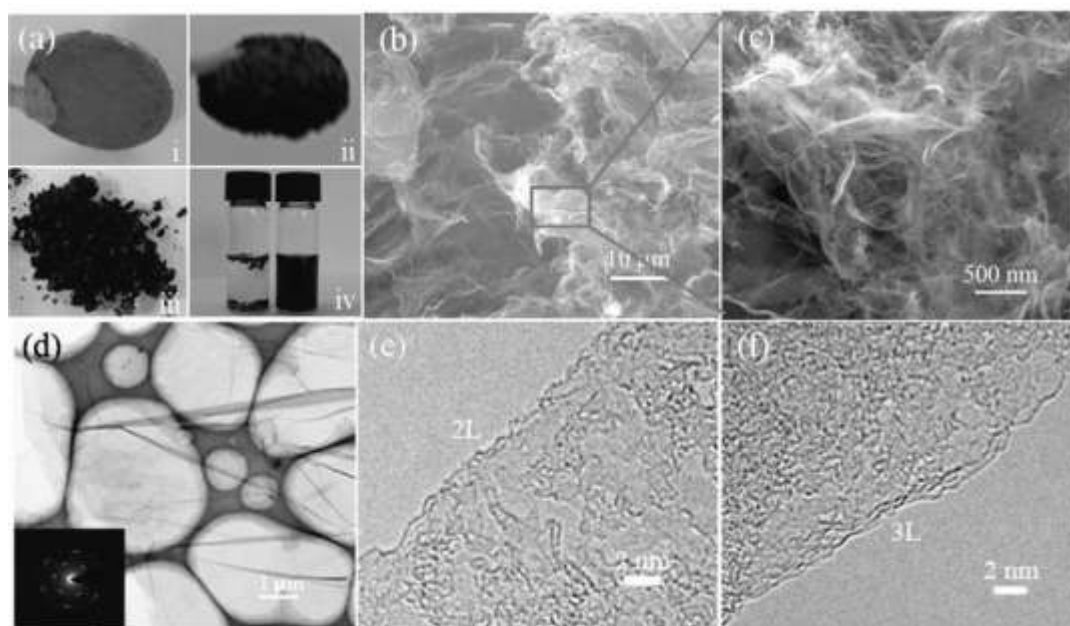


**Figure 1.4:** i) Images of EG electrodes; ii) images of EG after EIE; iii) images of Few Layer Graphene powder; and iv) EG and FLG dispersions in NMP. (b) and (c) are SEM pictures of freshly crafted FLG granules. d) FLG diffraction pattern caused by electrons and TEM picture. HR-TEM pictures of graphene sheets showing the bilayer and trilayer edges are shown in figures e and f.

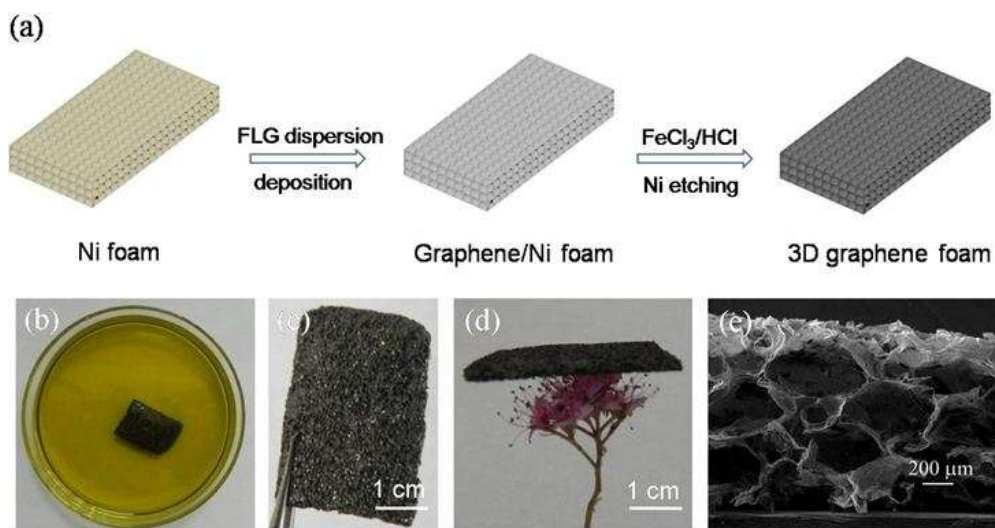


**Figure 1.5:** A Diagram showing the steps for fabricating GF utilising Ni foam as a template for self-sacrifice and  $\text{FeCl}_3/\text{HCl}$  solutions as an etchant (A). Images of a graphene/Ni foam that has been submerged in a solution of  $\text{FeCl}_3$  and  $\text{HCl}$  (1 M/1 M) to remove Ni (B), GF (C), and GF on a flower (D).

Additionally, these graphenenanosheets have a mean thickness of two to four layers. In relation to the total amount of starting EG, more than 75% of the graphenenanosheets had a thickness of fewer than seven layers, according to the statistical analysis of our AFM and TEM observations and this yield of the exfoliated

graphenenanosheets (>90%). These graphenenanosheets typically have lateral sizes between 10 and 30  $\mu\text{m}$ . The crystalline nature of the freshly generated graphenenanosheets was examined using Raman spectroscopy [7,29,30]. A sharp G peak at 1581  $\text{cm}^{-1}$ , a faint D band at 1336  $\text{cm}^{-1}$ , a D' shoulder peak at 1617  $\text{cm}^{-1}$ , and a 2D band at 2700  $\text{cm}^{-1}$  may all be seen, as shown in Fig.1.6C. Take note that the Raman spectra of EG lack the D and D' bands. The intensity ratio of D to G bands (ID/IG), which is around 0.30, indicates that there may have been some abnormalities in the graphenenanosheets; these may have been brought on by the exfoliation process. The chemical makeup of the as-obtained graphenenanosheets was investigated using X-ray photoelectron spectroscopy (XPS).

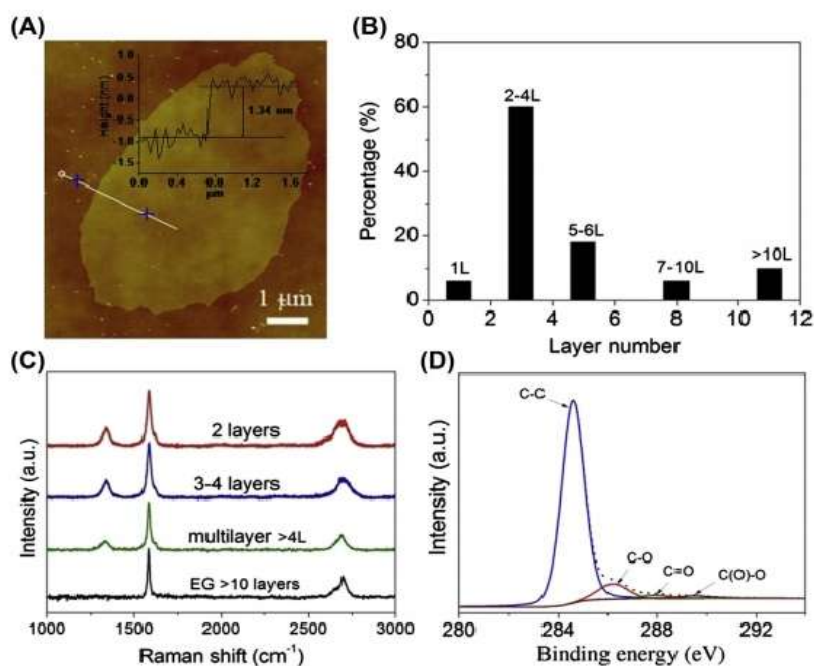


**Figure 1.6A:** FLG coated on a silicon substrate as seen in an atomic force microscope image (A). According to a bilayer statistical thickness distribution histogram of the FLG sheets as they were prepared (B), the thickness is around 1.34 nm. 92 randomly chosen sheets in total were used for AFM characterisation. Raman spectra of EG (C) and FLG flakes of varying thicknesses. FLG (D) C1s X-ray photoelectron spectroscopy spectrum.

- 2. Anode and Cathode Based on Three-Dimensional Ni/GrapheneHybrid Foam for Flexible Supercapacitors:** MnO<sub>2</sub>/HGNF// Polyaniline, was fabricated by using in situ electrochemical technique. SEM images shows that the NF featured a 100 $\mu\text{m}$  thickness and a 3D porous structure. and linked the network of conductivity and graphenenanosheets in the HGNF supplied an abundance of electron and ion transport channels. HGNF offered 5.1  $\Omega\text{sq}^{-1}$  of sheet resistance, as determined by a four-probe technique. **Fig.1.7** displays the 10 cycles of cv curves at a scan rate of 50  $\text{mV s}^{-1}$ . For the first cycle, there was an oxidation peak at 0.88 V, which was caused by the transformation of Mn<sup>2+</sup> into MnO<sub>2</sub>. Additionally, for both NF and HGNF, the peak potential shifted from a negative to a positive value the scan interval extended. It is simple to see the striking between the NF and HGNF, there is a variation in electrochemical surface activity

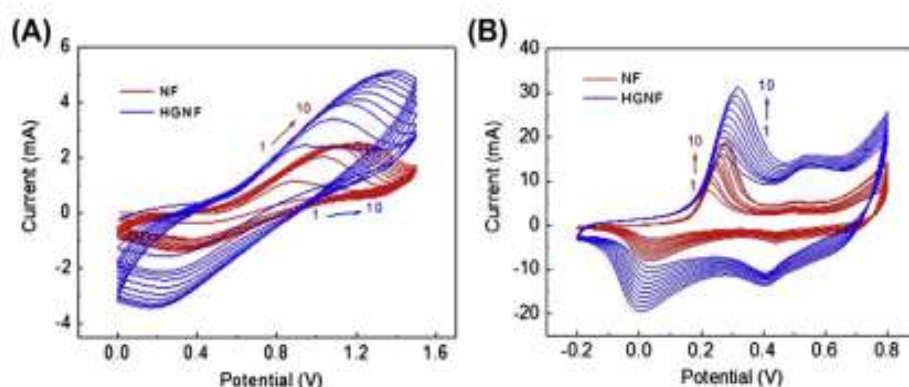


**Figure 1.7:** CV at a scan rate of 50 mV s<sup>-1</sup> for 10 cycles

When compared to electrodeposition on NF alone, the ultimate current dramatically enlarged as electrodeposition progressed on HGNF. The MnO<sub>2</sub> had been accumulated on the outermost layer of the GF of the HGNF was what caused the sudden increase in current density. The adsorption, transporting ions and electrons after desorption were significantly influenced by the GF micro/mesopores in HGNF [31,32]. These findings thus demonstrate that the 3D HGNF framework with 2D graphene micro/mesopores had advantages over Adsorption and transit of electronic and ions, resulting in a greater apparent current thickness. Compared to NF and GF, HGNF demonstrated superior electrochemical efficiency in terms of the deposition current

SEM and TEM were used to describe MnO<sub>2</sub>/NF, PANI/NF, MnO<sub>2</sub>/HGNF, and PANI/HGNF geometries. On the surface of MnO<sub>2</sub>/NF, MnO<sub>2</sub> organized into densely packed nanorods at random. Transmission Electron Microscopic results confirmed that MnO<sub>2</sub> was composed of numerous dense, syringe-shaped nanorods that were in close contact with graphene nanosheets. PANI nanoribbons were used to create the porous PANI film, which was then covered in graphene sheets. The MnO<sub>2</sub> nanoneedles have a diameter of approximately 5 nm. The PANI nanorod has a diameter of approximately 150 nm. A three-electrode setup with a Pt foil and an Ag/AgCl as the counter and reference electrodes in 1 M Na<sub>2</sub>SO<sub>4</sub> aqueous electrolyte was used to analyse the electrochemical characteristics of the MnO<sub>2</sub>/HGNF and PANI/HGNF, respectively, in their prepared states. By using CV and CC measurements, the specific capacitance of the nanocomposites as-prepared was determined.

The MnO<sub>2</sub>/HGNF's triangular CC curves and rectangle CV curves are depicted in Fig. 1.8A and C, respectively, with a potential between 0 and 0.8 V. In the potential range between 0.8 to 0 V, the PANI/HGNF's CV curves in a rectangle and CC curves in a triangle are depicted in Figs. 1.8 B and D, respectively. Thus, the charge storage at 1A/g current density capacities of the Electrodes made of PANI/HGNF and MnO<sub>2</sub>/HGNF were both considerably higher (192.0 F g<sup>-1</sup>) than that of the HGNF electrode, showing an improved influence of HGNF. The cycling experiments on the MnO<sub>2</sub>/HGNF and PANI/HGNF electrodes were completed after 2000 cycles at a current density of 2A/g, revealed 84% and 81% of the capacitance retained. MnO<sub>2</sub>/HGNF and PANI/HGNF electrodes had charge transfer resistances of 8.2 and 5.1Ω, respectively, as shown by the EIS curves in Fig. 1.8 F, demonstrating the excellent conductivity of HGNF.



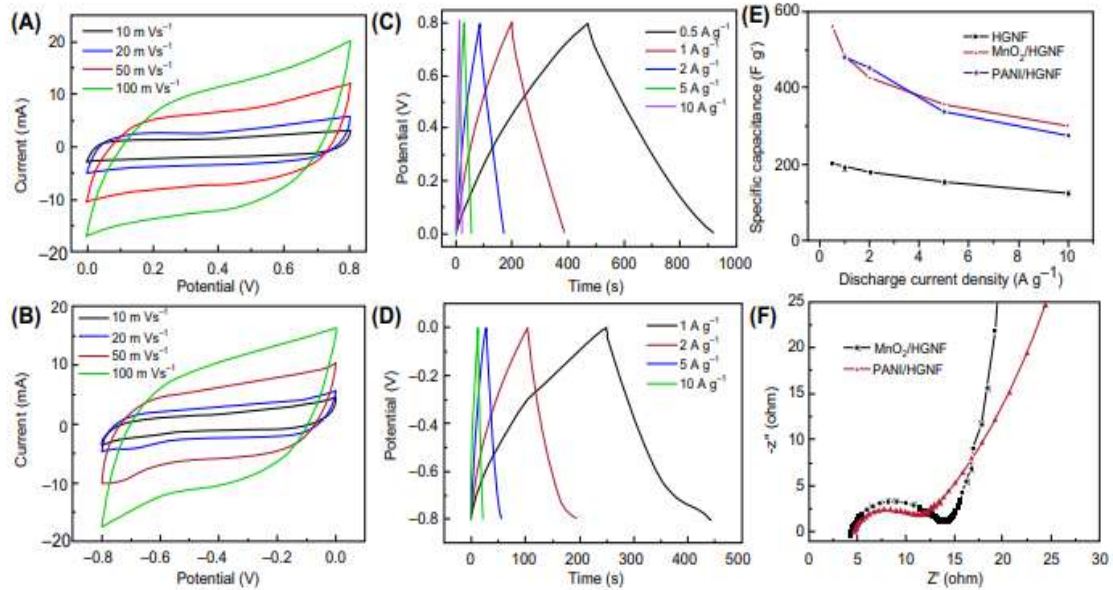


**Figure 1.8:** CV curves of MnO<sub>2</sub>/HGNF (B) CV curves of PANI/HGNF). Charge-discharge curves of MnO<sub>2</sub>/HGNF and PANI/HGNF electrodes Fig.(C,D). (E) Dependence of HGNF, MnO<sub>2</sub>/HGNF, and PANI/HGNF electrodes' specific capacitance (F) PANI/HGNF and MnO<sub>2</sub>/HGNF Nyquist graphs

#### IV. CONCLUSION

The possibility for flexible supercapacitors with high performance was established using 2D and 3D graphene and other 2D inorganic nanomaterials. Ion intercalation pseudocapacitance, redox, and electric double-layer capacitance working together synergistically to boost capacitance, rate performance, and cycling stability. Studies on graphene-based and inorganic 2D nanomaterials have shown that porous nanosheets that permit quick ion transport down channels and across nanosheets produce the best energy storage. It has been demonstrated that designing 3D hierarchical structures using 2D and other nanomaterials improves the efficiency of energy storage. The widespread storage of energy using 2D nanomaterial technologies still faces various obstacles. Ion transport is constrained by 2D nanomaterials' weak electric conductivity and propensity to stack. Hybridization can be used to solve those issues. It is important to consider new 2D nanomaterials' durability, suitability for appropriate electrolytes in broad electrochemical panels that permit an increased energy density, and the design of compatible electrode/electrolyte edges while doing research on or creating new 2D nanomaterials.

#### REFERENCES

- [1] Xinheng Li, Liqiong Wu, et al. Emerging 2D Nanomaterials for Supercapacitor Applications. *Emerging Materials for Energy Conversion and Storage* (2018) 155-183.
- [2] K.S. Novoselov, A.K. Geim, et al., Two-dimensional gas of massless Dirac fermions in graphene, *Nature* 438 (2005) 197.
- [3] K.S. Novoselov, A.K. Geim, et al., Electric field effect in atomically thin carbon films, *Science* 306 (2004) 666.
- [4] S. Pisana, M. Lazzeri, et al., The rise of graphene, *Nat. Mater.* 6 (2007) 198.

- [5] Y. Zhang, Y.-W. Tan, et al., Experimental observation of quantum hall effect and Berry's phase in graphene, *Nature* 438 (2005) 201.
- [6] X. Li, W. Cai, et al., Large-area synthesis of high quality and uniform graphene films on copper films, *Science* 324 (2009) 1312.
- [7] S. Bae, H. Kim, et al., Roll-to-roll production of 30-inch graphene films for transparent electrodes, *Nat. Nanotechnol.* 5 (2010) 574.
- [8] Q. Yu, L.A. Jauregui, et al., Control and characterization of individual grains and grain boundaries in graphene grown by chemical vapour deposition, *Nat. Mater.* 10 (2011) 443.
- [9] J.R. Miller, R.A. Outlaw, et al., Graphene double-layer capacitor with ac line-filtering performance, *Science* 329 (2010) 1637.
- [10] Y. Hernandez, V. Nicolosi, et al., High-yield production of graphene by liquid-phase exfoliation of graphite, *Nat. Nanotechnol.* 3 (2008) 563.
- [11] K.R. Paton, E. Varrla, et al., Scalable production of large quantities of defect-free few-layer graphene by shear exfoliation in liquids, *Nat. Mater.* 13 (2014) 624
- [12] S. Stankovich, D.A. Dikin, et al., Synthesis of graphene-based nanosheets via chemical reduction of exfoliated graphite oxide, *Carbon* 45 (2007) 1558.
- [13] H.Wang, J.T. Robinson, et al., Solvothermal reduction of chemically exfoliated graphene sheets, simultaneous nitrogen doping and reduction of graphene oxide, *J. Am. Chem. Soc.* 131 (2009) 9910.
- [14] K. Haubner, J. Murawski, et al., The route to functional graphene oxide, *ChemPhysChem* 11 (2010) 2131
- [15] E. Benavente, M.A. Santa Ana, et al., Intercalation chemistry of molybdenum disulfide, *Coord. Chem. Rev.* 224 (2002) 87.
- [16] Z. Zeng, Z. Yin, et al., Single-layer semiconducting nanosheets: high-yield preparation and device fabrication, *Angew. Chem. Int. Ed.* 50 (2011) 11093.
- [17] C.C. Mayorga-Martinez, A. Ambrosi, et al., Transition metal dichalcogenides (MoS<sub>2</sub>, MoSe<sub>2</sub>, WS<sub>2</sub> and WSe<sub>2</sub>) exfoliation technique has strong influence upon their capacitance, *Electrochem. Commun.* 56 (2015) 24.
- [18] G. Eda, H. Yamaguchi, et al., Photoluminescence from chemically exfoliated MoS<sub>2</sub>, *Nano Lett.* 11 (2011) 5111.
- [19] M.Chhowalla, H.S. Shin, et al., The chemistry of two-dimensional layered transition metal dichalcogenidenanosheets, *Nat. Chem.* 5 (2013) 263.
- [20] M. Pumera, Z. Sofer, et al., Layered transition metal dichalcogenides for electrochemical energy generation and storage, *J. Mater. Chem.* 2 (2014) 8981.
- [21] Z. Chen, W. Ren, et al., Three-dimensional flexible and conductive interconnected graphene networks grown by chemical vapour deposition, *Nat. Mater.* 10 (2011) 424.
- [22] H.X. Ji, L.L. Zhang, et al., Ultrathin graphite foam: a three-dimensional conductive network for battery electrodes, *Nano Lett.* 12 (2012) 2446.
- [23] X.-C. Dong, H. Xu, et al., 3D graphenecobalt oxide electrode for high-performance supercapacitor and enzyme less glucose detection, *ACS Nano* 6 (2012) 3206.
- [24] C. Shan, H. Tang, et al., Facile synthesis of a large quantity of graphene by chemical vapor deposition: an advanced catalyst carrier, *Adv. Mater.* 24 (2012) 2491.
- [25] J.-S. Lee, H.-J. Ahn, et al., Three-dimensional nano-foam of few-layer graphene grown by CVD for DSSC, *Phys. Chem. Chem. Phys.* 14 (2012) 7938.
- [26] S.Berbethmary,K.Nalini,K.Rajalakshmi,Synthesis,Characterisation and thermoelectric properties of Ca substituted nanostructured SrMnO<sub>3</sub> by sol-gel hydrothermal method,*Material Today:Proceedings*57(2022) 2344.
- [27] L. Wu, W. Li, et al., Powder, paper and foam of few-layer graphene prepared in high yield by electrochemical intercalation exfoliation of expanded graphite, *Small* 10 (2014) 1421.
- [28] L. Wu, L. Hao, et al., MnO<sub>2</sub> nanoflowers and polyanilinenanoribbons grown on hybrid graphene/Ni 3D scaffolds by in situ electrochemical techniques for high performance asymmetric supercapacitors, *J. Mater. Chem.* 5 (2017) 4629
- [29] Y. Huang, J. Liang, et al., An overview of the applications of graphene-based materials in supercapacitors, *Small* 8 (2012) 1805.
- [30] Y. Chen, X. Zhang, et al., High performance supercapacitors based on reduced graphene oxide in aqueous and ionic liquid electrolytes, *Carbon* 49 (2011) 573.
- [31] J.S. Huang, B.G. Sumpter, et al., A universal model for nanoporous carbon supercapacitors applicable to diverse pore regimes, carbon materials, and electrolytes, *Chem. Eur J.* 14 (2008) 6614.
- [32] C.-H. Huang, Q. Zhang, et al., Three-dimensional hierarchically ordered porous carbons with partially graphitic nanostructures for electrochemical capacitive energy storage, *ChemSusChem* 5 (2012) 563